RESEARCH ARTICLE | MAY 15 2023

Dynamic wetting properties of PDMS pseudo-brushes: Four-phase contact point dynamics case

Special Collection: Chemical Physics of Controlled Wettability and Super Surfaces

Peyman Rostami ; Mohammad Ali Hormozi ; Olaf Soltwedel ; Reza Azizmalayeri ; Regine von Klitzing; Günter K. Auernhammer

J. Chem. Phys. 158, 194703 (2023)
https://doi.org/10.1063/5.0142821

The Journal of Chemical Physics ARTICLE scitation.org/journal/jcp

Dynamic wetting properties of PDMS pseudo-brushes: Four-phase contact point dynamics case

Cite as: J. Chem. Phys. 158, 194703 (2023); doi: 10.1063/5.0142821
Submitted: 17 January 2023 • Accepted: 2 May 2023 •
Published Online: 15 May 2023

Peyman Rostami,[1,a)] Mohammad Ali Hormozi,[2] Olaf Soltwedel,[2] Reza Azizmalayeri,[1] Regine von Klitzing,[2,b)] and Günter K. Auernhammer[1,c)]

AFFILIATIONS

[1] Abteilung Polymergrenzflächen, Leibniz-Institut für Polymerforschung Dresden e.V., Dresden 01069, Germany
[2] Soft Matter at Interfaces, Department of Physics, Technical University of Darmstadt, Darmstadt 64289, Germany

Note: This paper is part of the JCP Special Topic on Chemical Physics of Controlled Wettability and Super Surfaces.
[a)] **Electronic mail:** rostami@ipfdd.de
[b)] **Electronic mail:** klitzing@smi.tu-darmstadt.de
[c)] **Author to whom correspondence should be addressed:** auernhammer@ipfdd.de

ABSTRACT

We investigate the wetting properties of PDMS (Polydimethylsiloxane) pseudo-brush anchored on glass substrates. These PDMS pseudo-brushes exhibit a significantly lower contact angle hysteresis compared to hydrophobic silanized substrates. The effect of different molar masses of the used PDMS on the wetting properties seems negligible. The surface roughness and thickness of the PDMS pseudo-brush are measured by atomic force microscopy and x-ray reflectivity. The outcome shows that these surfaces are extremely smooth (topologically and chemically), which explains the reduction in contact angle hysteresis. These special features make this kind of surfaces very useful for wetting experiments. Here, the dynamics of the four-phase contact point are studied on these surfaces. The four-phase contact point dynamics on PDMS pseudo-brushes deviate substantially from its dynamics on other substrates. These changes depend only a little on the molar mass of the used PDMS. In general, PDMS pseudo-brushes increase the traveling speed of four-phase contact point on the surface and change the associated power law of position vs time.

I. INTRODUCTION

In polymer brushes, the polymer chains are irreversibly (and uniformly) grafted to the substrate and stretched away from the substrate to minimize the chance of overlapping.[1] Preparing polymer pseudo-brushes is an alternative way for obtaining a strongly adsorbed layer of polymer chains on a surface.[2–4] These pseudo-brushes are nanometric coating layers on top of different substrates (such as glass or metal oxide), applying these pseudo-brushes is easy and do not require special methods or equipment.[5–8]

The wetting properties of pseudo-brushes play an important role in extensive applications from adhesion[9] and lubrication[10] to coating applications.[11] Using Polydimethylsiloxane (PDMS) pseudo-brushes or PDMS brushes is one of the long-time stable methods to make water repellent surfaces with low contact angle hysteresis.[4,12] The low contact angle hysteresis is commonly explained by the smoothness of brushes as well as the flexibility of PDMS.[13] Since the PDMS is flexible, it might be able to coat the substrate more efficiently. In terms of robustness, these surfaces are very stable that by storing in a vertical position for two weeks not only the contact angle hysteresis remained constant but also no dry out is observed.[12] By changing the molar mass of the used PDMS, it is possible to change the physico-chemical properties of surfaces, e.g., the brush height and wetting properties.[14]

Despite the fact that in many hydrodynamic explanations (theoretical and numerical simulation) of the drop's movement, the contact angle hysteresis is assumed zero, just in recent years, the low contact angle hysteresis surfaces are studied experimentally.[15,16] The behavior of a drop on a substrate depends on the properties of the substrate and interactions at the liquid–solid interface. When the

substrate is flat, smooth (zero topographical roughness), and chemically homogeneous, zero contact angle hysteresis condition can be assumed.[17] Contradictory, others observed contact angle hysteresis on really smooth substrates.[18,19] They correlate the contact angle hysteresis to the disjoining pressure.[20,21] In reality, all the surfaces have topographical roughness as well as chemical heterogeneity. By using atomic force microscopy (AFM imaging), it is possible to measure the topographical and chemical roughness of the surfaces. The minimum size of roughness needed to introduce contact angle hysteresis is in the range of the size of a few molecules.[22] Also, chemical heterogeneity of surfaces will lead to higher contact angle hysteresis.[23]

PDMS pseudo-brush softens the surface, i.e., introduces a certain deformability of the surface. It is known that the softness of the substrate has a considerable effect on the motion of the three-phase contact line. As a result, softer surfaces lead to slower contact line dynamics.[24] The wetting behavior on soft gels or elastomers is well described, and it is possible to get the detailed shape of the drop and the deformation of the soft substrate.[24] This information allows correlating the shape and contact line velocity to the mechanical properties of solid bulk.[25] In the case of PDMS pseudo-brushes, we have a nanometric layer of a soft material on a solid bulk with high stiffness (e.g., glass). This topmost nanometric layer has a significant impact on wetting dynamics. We differentiate three regimes in the wetting of soft substrates: (i) the quasi-static one, in which the substrate deformation is independent of the (small) contact line speed, (ii) the slow dynamic regime in which the ridge height and shape depend on contact line speed,[26] and (iii) the very fast dynamic regime in which the wetting seems to be independent of any ridge.[25] In the fast wetting situation [regime (iii)] on the soft substrates, if the contact line velocity is high enough the substrate cannot form a wetting ridge and the relevant parameters are the quasi-static wetting properties, such as contact angle hysteresis. Based on these facts, to understand the regime (iii), it is crucial to study the quasi-static wetting properties of these substrates. Surprisingly the fast wetting dynamics (such as four-phase contact point dynamics) on these PDMS pseudo-brushes are not well studied.

To study the structural properties of these pseudo-brushes, Atomic Force Microscopy (AFM) and specular X-Ray Reflectivity (XRR) are used. AFM is a unique method that can be employed for the high-resolution characterization of polymer brushes in terms of surface morphology,[27] brush thickness,[28] nanomechanical properties,[29] and their dynamic behavior.[30,31] The working principle of AFM and the application of different operational modes in polymer brush characterization are already presented in the literature;[32] therefore, the details are not mentioned here. Using AFM topography scanning, it is possible to resolve the structure of brushes with high spatial resolution. Sakurai *et al.*[28] employed AFM to investigate the morphology and wettability of looped PDMS brushes grafted on Si substrate. In another study, Motornov *et al.*[33] used tapping mode AFM to image hybrid PDMS-EPEI (ethoxylated polyethylenimine) brushes in both water and air environment. They showed that the wettability of these brushes is switched from hydrophobicity in the air to hydrophobicity when it is in contact with water. We employed specular x-ray reflectivity (XRR) to measure the pseudo-brush thickness. As a non-destructive method, this technique allows us to refine the lateral averaged electron density profile along the surface normal with sub-nm resolution.

Drop merging of non-identical drops plays an essential role in many industrial applications from printing technology to metallurgy.[34–36] When two immiscible drops with different surface tensions come to contact, the drop with lower surface tension engulfs the other drop.[37] Under such circumstances, the drop with lower surface tension wets the contact line of the other drop. As a result, a point is formed, which is the contact point of two liquids on the solid substrate in a gas atmosphere, and this point is called the four-phase contact point.[37] The statics of the four-phase contact point was observed in metallurgy phenomena.[38] Despite its relevance for many applications (e.g., metallurgy and drop encapsulation), the dynamics of the four-phase contact point has been studied only recently. It was shown that the four-phase contact point dynamics follows the general roles of the famous Lucas–Washburn equation for capillary filling problem $[H(t) = D\sqrt{t}]$.[39–41] In Lucas–Washburn equation, the penetration coefficient (D) is a function of surface tension (γ) to viscosity (η) ratio, the wettability (θ), and the diameter of the capillary (r),

$$D = \sqrt{\frac{\gamma r \cos(\theta)}{2\eta}}. \tag{1}$$

Later, we showed that the general parameters for four-phase contact point dynamics are the same as the modified version of the Lucas–Washburn equation for the V-shape groove.[37] We found the dependency of the four-phase contact points to (i) the surface tension to viscosity ratio, (ii) the opening angle of the groove (the contact angle of the first drop), (iii) the viscosity of the first drop (the friction between two drops),[37]

$$D = \sqrt{\frac{l_0 K(\gamma, \alpha, \theta_1, \theta_2)}{4\pi\eta_{\text{eff}}}}, \tag{2}$$

where l_0 is the depth of the groove, K is a function of surface tension γ, the opening angle of groove α and the contact angle of two liquids on the surface (θ_1, θ_2), and the effective viscosity is η_{eff}. In general, it is shown that by increasing the surface tension to viscosity ratio, decreasing the opening angle (increasing the first drop contact angle), and/or decreasing the first drop viscosity, the movement of the four-phase contact point speeds up. Although the drop mobility, e.g., low contact angle hysteresis, is very important in many applications, such as coating, this effect on the four-phase contact point is still unstudied.

There are three major categories of substrates with the same macroscopic contact angles soft coating (PDMS pseudo-brushes), hard coating (silanized substrates), and soft material (PDMS thick layer). In this study, we focused on the wetting behavior on two first categories, the PDMS pseudo-brushes (e.g., a nanometric layer of PDMS on top of the solid substrate) and silanized substrate for two cases of three-phase contact line and four-phase contact point. One of the main open questions is, what are the structural properties of these pseudo-brushes such as the surface morphology and thickness? We address this question with the AFM method, which is employed to measure the topographical and chemical roughness of substrates and XRR to measure the brush thickness. Furthermore, we investigate the influence of the strongly decreased contact angle hysteresis on the drop merging dynamics. We are looking at the effect of low

contact angle hysteresis induced by pseudo-brushes on the complex and unique dynamic of four-phase contact point. In the current work, not only the physical properties of working liquids but also the properties of the surface are studied.

II. MATERIALS AND METHODS

The process for preparing these PDMS pseudo-brushes is well explained in the literature,[12] so we only briefly explain it here. The first step is to clean the substrates (Thermo Scientific Menzel-Gläser, Microscope Slides, 26×76 mm^2) for the four-phase contact point experiments or silicon wafers (SK Siltron, boron-doped, 100 oriented, double side polished, 300 mm diameter 0.75 mm thick) for AFM and x-ray studies. The substrates are cleaned by immersing them in tetrahydrofuran (Acros Organics Co. 99.6%), acetone (Fisher Scientific Co. 95%), and isopropanol (Fisher Scientific Co. ~ 95%) and applying ultrasound (VWR Ultrasonic Cleaner Co. USC-TH) for 15 min in each liquid. PDMS polymer melts were purchased from Gelest, Inc. and used without any further modification. Then a thin film of the polymer melt of the chosen molar mass is placed on the substrate (Table I) using the drop-casting method. Subsequently, the substrates are heated up to curing temperature T_{cu} and backed for 4 min. The sample names are based on the commercial names and correlated with the molar mass of silicon oil (Table I).

To keep the duration of coating constant at 4 min, different curing temperatures were selected for different molar masses. The effect of different curing temperatures on the brush thickness was not explored systematically. Nevertheless, the DMS-T21 sample, which is cured at 230 °C, had nearly identical scattering length density (SLD) profiles (i.e., thickness). In the end, the substrates are washed with acetone, isopropanol, and ultra-pure water to remove unbounded PDMS chains. The contact angle of a seated water drop (deposited on the substrate and not spreading anymore) on such a surface is around 90°; see also below for quantification and discussion of the contact angle hysteresis. To be able to compare these substrates with substrates without pseudo-brushes, we prepared hydrophobic substrates using small molecules. The cleaned substrates are treated for 10 min in the plasma cleaner device (PlasmaFlecto 10, Plasma Technology GmbH) to activate the surface. Immediately after plasma treatment, the substrates are placed in a closed glass desiccator that has 30 μl of 1H, 1H, 2H, 2H-perfluorooctyltriethoxysilane (Sigma-Aldrich Co. 97%). The container was incubated in the oven for 9 h at 100 °C. The contact angle of a seated water drop on a hydrophobic surface is also in a range of $90^\circ \pm 5^\circ$. From now on, we name these substrates silanized substrates.

For the wetting experiments, water, glycerin (Sigma-Aldrich Co. 99%), and mixtures thereof as well as bromocyclohexane (Sigma-Aldrich Co. 99%), bromocyclopentane (Sigma-Aldrich Co. 99%), and bromocycloheptane (Sigma-Aldrich Co. 99%) are used as the operating liquids (Table II). In this study, the water, glycerin, and their mixtures are classified as high surface tension liquids and bromocyclohexane, bromocyclopentane, and bromocycloheptane as low surface tension liquids. The wetting behavior of each class of liquids is studied separately and later both classes are used to study the dynamics of the four-phase contact point. To measure the contact angle hysteresis, we performed the tilted substrate experiments on OCA15 (Data physics Co.) instrument. OCA15 enables us to tilt the surface with the accuracy of 0.1°. Our approach to measuring the contact angle hysteresis is to tilt the substrate with a defined angle (α). The drop falls from a low height (0.5 cm) on the tilted substrate. In this situation, the kinetic energy due to the drop fall is negligible (details can be found in the supplementary material). After a few millimeters, the drop reaches a steady velocity and constant dynamic contact angles. For the low-height cases (<1 cm), the contact angle hysteresis remains constant, and just by increasing the height, the nonzero kinetic energy has an impact on the drop sliding.

To measure the four-phase contact point dynamics, we follow the drop merging with a custom-made setup. The setup has a high-speed camera (FASTCAM Mini AX 200 Photron Co.) to observe the process from the top view (see Fig. 1). First, the drop with higher surface tension is placed and then the second drop is deposited next to that. The distance between the two drops is chosen such that the spreading drop (drop with lower surface tension) touches the other drop very gently. In all experiments, the volumes of the first and second drops are approximately equal.[37] The camera is equipped with Navitar objective with up to 12× magnification with a 2× F-mount adapter, having a field of view of 17.5 mm at 1000 frames per second. The test section is illuminated by a LED lamp (SCHOTT KL 2500) along with a diffuser sheet to have homogeneous backlight. During experiments, the relative humidity and the temperature were kept constant (relative humidity 48% ± 3% and a temperature 23.0 ± 0.5 °C). To avoid any vibration, the test section was placed on a thick marble stone (20 cm). Additionally, all possible sources of vibrations (e.g., the camera) were mechanically disconnected from this stone plate.

Pseudo-brush roughness measurements were performed using the Cypher AFM system (Asylum Research, Santa Barbara, CA, USA). The cantilever for all measurements was OMCL-AC200TS (Olympus, Tokyo, Japan) with an average spring constant of 9 $\frac{N}{m}$ and resonance frequency of 150 kHz in air. All measurements were conducted in intermittent contact (tapping mode) as the operational

TABLE I. Properties of PDMS; M_N as average molar mass (supplier's data), ν as kinematic viscosity of polymer melt, N as polymerization index,[42] and T_{cu} is the curing temperature of each sample.

Sample	$M_N(\frac{g}{mol})$	ν (cSt)	N	T_{cu} (°C)
DMS-T5	770	5	9	210
DMS-T21	5 970	100	79	245
DMS-T25	17 250	500	232	285

TABLE II. Properties of used liquids.

Chemicals	Surface tension ($\frac{mN}{m}$)	Viscosity (mPa s)
Water	72.1 ± 0.1	0.9321
Glycerin	63.5 ± 0.1	1078
Bromocyclopentane	33.2 ± 0.1	1.4 ± 0.05
Bromocyclohexane	32.1 ± 0.1	2.2 ± 0.05
Bromocycloheptane	31.5 ± 0.1	3.9 ± 0.05

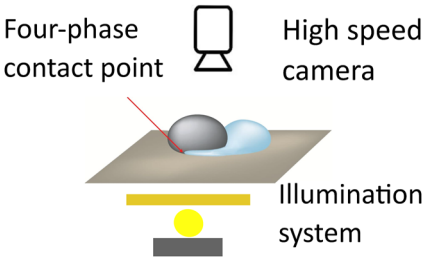

FIG. 1. Sketch of four-phase contact point setup: the solid substrate, high-speed camera, and illumination system. The four-phase contact point is shown.

mode and in the ambient condition. Also, this mode of measurement provides information on the energy dissipation during tip/sample interaction in the phase channel, which corresponds to the chemical homogeneity of the sample.

To determine the brush thickness, we employed XRR (x-ray reflectivity) using a Bruker D8 Advanced, equipped with a CuKα anode (λ = 1.54 Å). The procedure is thoroughly explained in the supplementary material. These measurements are done on silicon wafers, since the glass substrates are too wavy and we could not perform the XRR measurements on them, and on the other hand for four-phase contact point experiments, we needed a transparent substrate so we did wetting-related measurements on glass.

III. PDMS PSEUDO-BRUSHES ROUGHNESS AND THICKNESS

First, we study the structural properties of the PDMS pseudo-brushes. Tapping mode AFM is used for measuring the average roughness of PDMS pseudo-brushes. All measurements are conducted in a relatively high identical set-point regime (80% of target amplitude) where the repulsive forces are dominant. This setting avoids possible manipulation of the sample through the tip–surface interaction and provides information about surface topography with the highest spatial resolution. The scanning area is kept constant at $5 \times 5\ \mu m^2$, and each measurement was repeated at three different locations to obtain a mean value of the rms roughness. While the average roughness of a bare glass substrate is around 2 ± 0.2 nm, it drops to 247 ± 10 and 262 ± 13 pm for DMS-T5 and DMS-T21 PDMS pseudo-brushes, respectively. The typical AFM images for the DMS-T5 substrates are presented in Fig. 2(a). The corresponding phase image for the same sample is also plotted in Fig. 2(b). The phase diagrams clearly show a minimum lag in phase signal during measurement for PDMS pseudo-brushes. This can lead to the conclusion that PDMS pseudo-brush not only makes the surface physically smoother but also more chemically homogeneous. The AFM measurements for other samples are presented in the supplementary material.

Specular x-ray reflectivity is employed to investigate the vertical electron density profile of the PDMS pseudo brushes, namely, thickness and roughness. The measurements and fit results are displayed in Fig. 3. The brush thickness increases with increasing polymer weight (as seen from the rising oscillation frequency). Moreover, the observation of oscillations up to $Q_z = 0.4$ Å^{-1} indicates a very smooth interface. Beyond this *ad hoc* inspection, a common satisfactory qualitative analysis, as described in the methods section, required a three layers (first, second, third) model with some constraints between the fitting parameters. Here, we will try to give them a physically meaningful interpretation starting from the Si interface. The exact parameters are summarized in Table III.

- First layer: With a thickness of 10–20 Å, a density close to the SLD_{Si}, and a rather rough *SLD* distribution, this inter-layer might be a result of (partially) PDMS-filled cracks of the uppermost Si-substrate that were created during the ultrasound cleaning process. Due to here nearly identical *SLD* of Si and SiO_2, we exclude the latter as origin. Since the extracted SLD-value ($\approx 15 \times 10^{-6}$ Å^{-2}) is well above the SLD of H_2O ($\approx 9.5 \times 10^{-6}$ Å^{-2}) predominate water incorporation in the early stage of the PDMS film growth has to be excluded as well.
- Second layer: The thickness increases from 10 to 50 Å with increasing molecular weight. At the same time, the *SLD* increases first drastically from 2.4×10^{-6} Å^{-2} to saturate at 8×10^{-6} Å^{-2}. The layer's roughness toward the adjacent third layer is atomically smooth having only 2 Å. We attribute the second layer mirrors a dense PDMS-brush.
- Third layer: The thickness increases from 35 to 50 Å with increasing molecular weight. At the same time, the *SLD* is similarly low at $1–1.5 \times 10^{-6}$ Å^{-2} and the *SLD* smears out toward at air interface, which we had to constrain for fitting. Most probably the third layer resembles domains of aggregated PDMS-oligomers on top of the brushes that are flat or coiled adsorbed (depending on the molecular weight). Since the fitting is realized by a superposition of *SLD* (rather than reflectivity) its origin is coherent, which concludes that the lateral dimension is less than 1 μm (lesser than the lateral coherence volume of the measurement) likely in the form of single chains are small bundles. From the *SLD*-ratio of the second and third layer, one can estimate the area fraction of the residual oligomers to 12.5%–18%. The layer thicknesses l_2 and l_3 from the heavier PDMS (samples T21 and T25) are very similar to each other.

The interpretation of the second and third layer confirms findings of a previous study of the same brushes.[43] The authors observed a bimodal thickness distribution of the PDMS-brushes $M_N = 5970\ \frac{g}{mol}$ for films annealed for 24 h (comparable to the sample DMS-T21). To be precise from histogrammed force–distance curves, they determined that 90% of the brushes have a thickness of 2.8 ± 1.1 nm and some 10% roughly 5.5 nm. To account for this in the SLD-parameterization, an additional layer on top of the dense PDMS-box (second) with 10% of its SLD and the same thickness has to be included. Indeed, we had to add this box to our x-ray analysis to gain satisfying fits. Much to our delight even the absolute values of both approaches are very similar. The brush thickness of the low molecular weight sample (DMS-T5) is with 1 nm close to the 2.3 nm reported by Eifert *et al.*;[12] however, they annealed their brushes for only 2–3 min at 300 °C instead of 9 h at 100 °C.

The effect of different curing temperatures on the brush thickness was not explored systematically. Nevertheless, DMS-T21 sample, which is cured at 230 °C, had nearly identical SLD-profiles. So

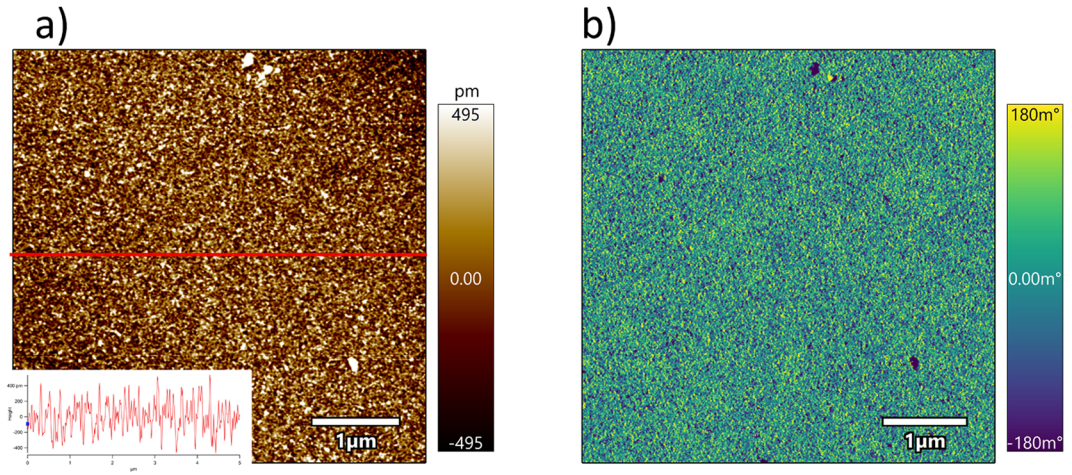

FIG. 2. (a) and (b) The height and phase image of the glass substrate coated with PDMS pseudo-brushes DMS-T5 ($770\,\frac{g}{mol}$). The cross section of each sample is shown in the inset of height image.

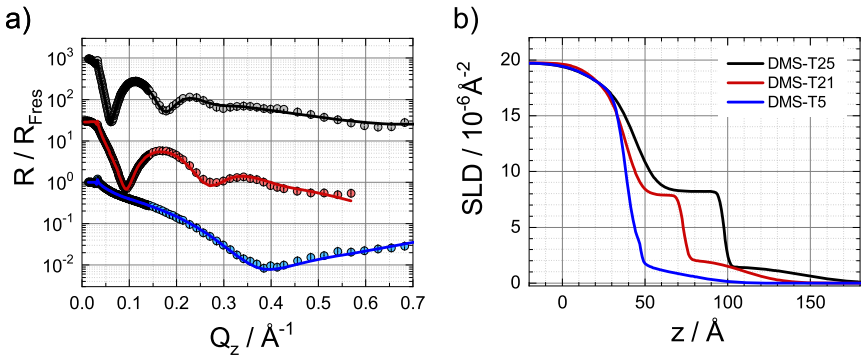

FIG. 3. *Fresnel*-normalized x-ray reflectivities (a) and corresponding refined scattering length density profiles (b). The measured reflectivity is the circles with error bars, which are mostly smaller than the symbol size. The fitted reflectivity (a) and their corresponding scattering length profiles (b) are the solid lines having the same color code. To enhance readability, the reflectivity curves are shifted by a factor of $\sqrt{1000}$ against each other. The Si-surface is set to $z = 0$ (b) and for increasing z the *SLD*-profiles first probe the interfacial layer and then bulk air.

far, the height of these pseudo-brushes is estimated or measured by ellipsometry technique[8,12,14] or AFM[43] so the current study reports better and more consistent data.

IV. CONTACT ANGLE HYSTERESIS OF PDMS PSEUDO-BRUSHES

We measure the advancing (θ_A) and receding dynamic contact angles (θ_R) of a drop on a tilted surface; see Materials and Methods for details. For low tilting angles, which cause low drop velocities ($V_{cl} \sim 0$), we measure the quasi-static advancing and receding contact angles. For the higher tilting angles, the dynamic effects come into account. The increase in the contact angle hysteresis ($CAH \sim \theta_A - \theta_R$) is due to the velocity-dependent contact angles. Since sometimes the contact angle hysteresis is measured based on the cosines of the angles (force) $CAH_c \sim \gamma(\cos\theta_R - \cos\theta_A)$, we give both values for the used substrates [Fig. 4(d)]. By measuring these contact angles as well as having the size of the drop and the tilting angle (α), one can write a force balance for the drop[44–46]

$$F = mg \sin\alpha = kw\gamma_L(\cos\theta_R - \cos\theta_A). \quad (3)$$

Here, m is the drop mass, g is the acceleration due to gravity, and k is a dimensionless constant that can be correlated with the shape of the drop having reported values between $\frac{1}{2}$ and $\frac{\pi}{2}$.[45,47–49] In the force balance equation [Eq. (3)], w, γ_L, θ_R, and θ_A are drop width, liquid surface tension, receding contact angle, and advancing contact angle, respectively. This equation shows that the smaller the tilting angle at which a continuous drop motion is observed, the lower the contact angle hysteresis has to be.

We performed experiments with water and bromocyclohexane on tilted substrates with different tilting angles α. When a water drop ($V = 30\ \mu l$) is placed on the tilted substrate, it starts rolling off on PDMS pseudo-brushes when $\alpha > 3.0°$. With increasing α, the

TABLE III. Fit parameters of the model fits shown in Fig. 3(a).

Sample DMS	σ_{Si} (Å)	l_1 (Å)	SLD_1 10^{-6} Å^{-2}	l_2 (Å)	SLD_2 10^{-6} Å^{-2}	σ_2 (Å)	l_3 (Å)	SLD_3 10^{-6} Å^{-2}
T5	18.6	9.5	14.71	9.5	2.35	0.9	34.1	1.04
T21	12.3	13.8	15.28	34.1	7.89	2.4	36.8	2.14
T25	18.3	18.9	15.46	52.5	8.22	2.2	47.2	1.50

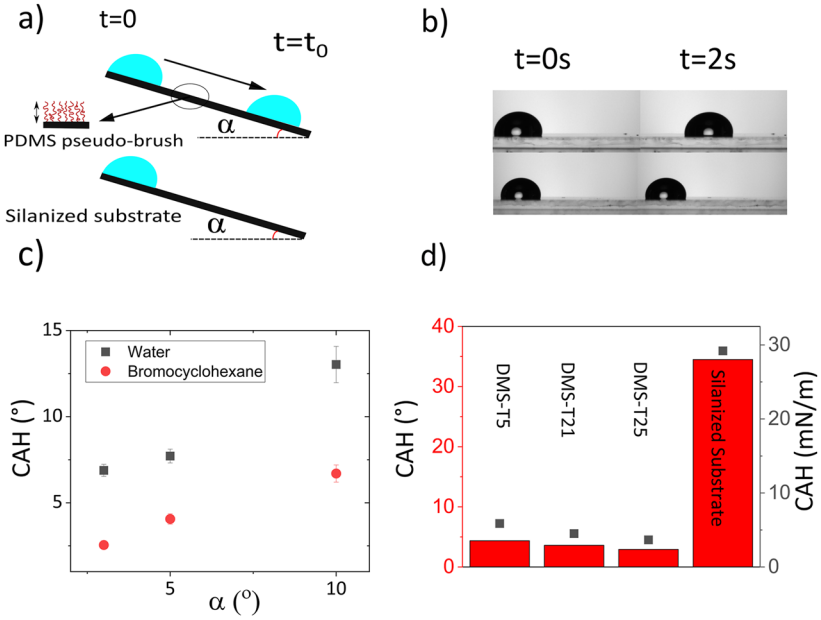

FIG. 4. (a) Sketch of the tilted substrate experiment. For low tilting angles of the substrates (α), the drop on the PDMS pseudo-brushes substrate rolls off easily but stays motionless on the silanized substrate. (b) Drop sliding of a water droplet (30 μl) on the tilted substrate ($\alpha = 5.0°$); top on PDMS pseudo-brushes (5970 $\frac{g}{mol}$) bottom on the silanized substrate. Note that the camera was tilted together with the substrate. (c) Contact angle hysteresis of water and bromocyclohexane drops on DMS-T5 (the PDMS pseudo-brushes with the molar weight of 770 $\frac{g}{mol}$) as a function of the tilting angle (α). (d) Contact angle hysteresis of water drop on different substrates. The tilting angle for PDMS pseudo-brushes is 3.0° and for silanized substrate is 30.0°. The mean value of advancing and receding contact angles are reported in the supplementary material.

drop velocity, as well as contact angle hysteresis, increases [Fig. 4(c)]. On the other hand, the water drop on the silanized substrate starts sliding only when the tilted angle is around 30.0°. This means that one needs ~10 times less force ($\frac{F_{Brush}}{F_{Silane}} = \frac{\sin \alpha_{Brush}}{\sin \alpha_{Silane}} = \frac{\sin 3°}{\sin 30°} = 0.104$) to move an identical water drop over PDMS pseudo-brushes rather than over a silanized substrate [Eq. (3)]. We attribute this huge difference to the surface not the hydrodynamic of the liquid.[50] The dynamics effect happens at relatively lower velocities. The bromocyclohexane drop slides even easier on the PDMS pseudo-brushes than water drop tilting angle 2.5° ± 0.5°. Approximately the same force ratio between PDMS pseudo-brushes and silanized substrate was found for bromocyclohexane drop as well. Even though the thickness of PDMS pseudo-brushes are different, their contact angle hysteresis of them are very close to each other at the same tilted angle ($\alpha = 3.0°$) [Fig. 4(d)]. By increasing the molar mass of the used PDMS, the contact angle slightly decreases.

This low contact angle hysteresis [high mobility of drops on the PDMS pseudo-brushes, Figs. 4(a) and 4(b)] illustrates the high homogeneity of the PDMS pseudo brushes. All mechanisms that might produce contact angle hysteresis (pinning) are weak in this case. We attribute this to the low melting and glass transition temperature of PDMS and the consequently high chain mobility in the pseudo-brush compare to the coating with small but less mobile perfluorooctyltriethoxysilane molecules. This observation stays true for all used liquids. To avoid any confusion, between the PDMS thick layers (which are normally used for soft wetting applications) with these PDMS pseudo-brushes, we compared the dissipated power in both cases. It is shown that the dissipated power is negligible compared to the thick PDMS layers (see the supplementary material).

V. FOUR-PHASE CONTACT POINT DYNAMIC

As described in previous studies[37,41] and the introduction, the dynamic of the four-phase contact point follows the same dynamic as the flow inside a V-shaped groove Figs. 5(a) and 5(b). The key parameters that have an impact on the four-phase contact point are (i) the surface tension to viscosity ratio, (ii) the opening angle of the groove (β), and (iii) the viscosity of the first drop. Based on these findings, the four-phase contact point dynamic model was developed [Eq. (2)].[37]

The aim of this section is to get deeper insight into the effect of the presence of PDMS pseudo-brushes (high mobile surfaces) on the four-phase contact point dynamics. Now the open questions are, what would happen if we change the properties of the solid wall (except the contact angle) while not changing the other relevant parameters? What would happen if we have a highly mobile surface? Does it change the dynamic of the four-phase contact point or just change the prefactors of the developed model [Eq. (2)]?

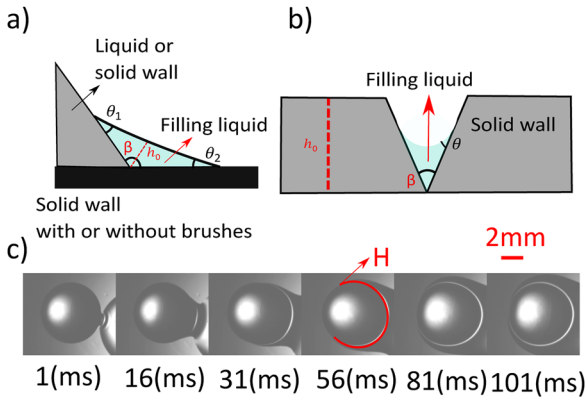

FIG. 5. (a) The cross section near the four-phase contact point illustrates the similarity to the V-groove. The four-phase contact point propagates perpendicular to this cross-sectional plane. The underneath wall is always solid with or without PDMS pseudo-brushes, the wall on the left side could be liquid (in case of the four-phase contact point) or solid (in case of a V-shape groove channel). (b) In the V-shape groove, the liquid contact angle is the same for both sides ($\theta_1 = \theta_2$), which can be different in the four-phase contact point situation. The opening angle of the V-shape groove (β) can be mimicked by changing the contact angle of the seated drop in the four-phase contact point case. h_0 shows the size of the groove. (c) The time series of drop merging for two drops on PDMS pseudo-brushes. The four-phase contact point forms and propagates around the first drop. The traveled distance of two four-phase contact points is marked as *H*.

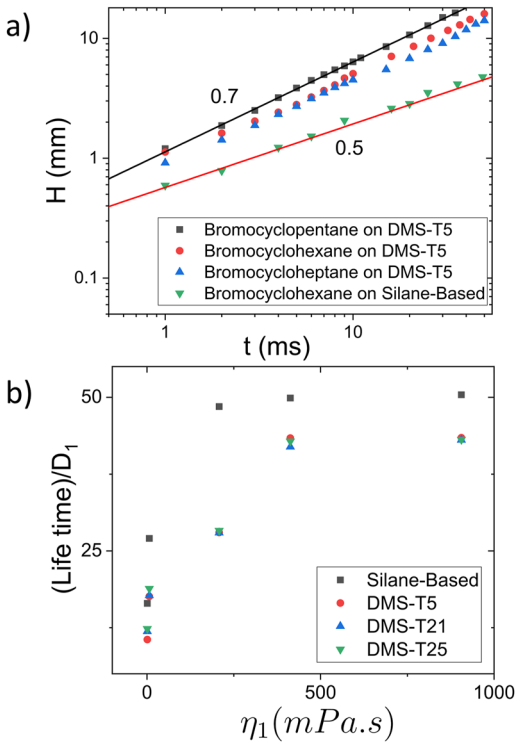

FIG. 6. (a) The length of the four-phase contact point (H) as a function of time for water as first drop and bromocyclopentane, bromocyclohexane, and bromocycloheptane on the DMS-T5 substrate and for bromocyclohexane on silanized substrate. (b) The lifetime of the four-phase contact point divided by the first drop diameter as a function of the first drop viscosity (η_1) for different substrates when the bromocyclohexane is the second drop.

To be able to answer open questions, we performed the experiments by changing the key parameters for four-phase contact point dynamics. Changing the contact angle of the first drop is not feasible since the PDMS pseudo-brushes have the same surface chemistry (and thus surface energy) independent of the thickness of the pseudo-brush or molar mass of the used polymer melt. The contact angle for a seated water drop (i.e., first drop) remains close to 90° for all of the substrates. The second relevant parameter is the ratio of surface tension to viscosity. This effect is plotted on the PDMS pseudo-brushes (DMS-T5) when the first drop is a water drop. The low surface tension drops (i.e., bromocyclopentane, bromocyclohexane, and bromocycloheptane) are used as a second drop (i.e., filling liquid). In the following discussion, we first focus on two observations (Fig. 6): (i) As for hard substrates,[37] by increasing this ratio, the four-phase contact point speeds up. (ii) The length of the four-phase contact point is not following the general Lucas–Washburn equation $[H(t) \approx Dt^{\frac{1}{2}}]$ anymore. In this case (water drop as the first drop), the length of the four-phase contact point (H) has a linear dependency to $\sim t^{0.7\pm0.03}$ [Fig. 6(a)]. The main reasons for this deviation from the Lucas–Washburn model that would be decreasing dissipation in the solid side and the moving of the first drop contact line. Reduction of dissipation on the solid side can increase the velocity of four-phase contact points since there is less pinning. Another point would be the fact that in this case (with PDMS pseudo-brushes) the contact line of the first drop is not pinned and moves during process (for water as the first drop ~100 μm). To decrease the movement of the first drop's contact line, one of the possibilities is increasing the viscosity of the first drop. To do so, we performed the measurements with an aqueous mixture of glycerin (with different concentrations) as the first drop and bromocyclohexane as the second drop. The results show that again, in this case, the time's exponent is well above the found exponent in the case of the silanized substrate (0.5 ± 0.05); see the supplementary material. As it is shown in the supplementary material, the exponent slightly decreases by increasing the viscosity of the first drop. As a result, the effect of movement of the contact line is a part of the explanation of why the time's exponent is different with solid substrates but it cannot explain the whole process.

Increasing the viscosity of the first drop reduces the speed of the four-phase contact point. A high viscosity contrast effectively transforms the liquid–liquid interface to a liquid–quasisolid interface.[37] Previously, we used the prefactor (D, coefficient of penetration) of the Lucas–Washburn equation $[H(t) \approx Dt^{\frac{1}{2}}]$ to compare the dynamics of the four-phase contact point in different scenarios, e.g., a function of the viscosity of the first drop. Here, the power law depends on the substrate (with and without PDMS pseudo-brush). To compare the different substrates, we use the lifetime of four-phase contact points, i.e., the difference between the start of drop coalescence and the end of drop engulfment. This is illustrated in Fig. 5(c), where it takes (100 ms) for the second drop to engulf the first drop, i.e., the lifetime of four-phase contact points for this case is (100 ms). We tried to keep the volume (subsequently

size) of the first drop in the same range for all of the measurements (60 ± 2 μl). But to be sure that the size of the drop does not have any influence, we divide the lifetime by the characteristic length of the drop (in this case, the diameter of the first drop diameter) and introduce the "normalized life time" for the rest of the paper.

With increasing the viscosity of the first drop, the normalized lifetime of the four-phase contact points increased [Fig. 6(b)]. This is equivalent to a slowing down of the four-phase contact points. Beyond a certain threshold, increasing the viscosity of the first drop will not change the filling rate of the liquid anymore. The viscosity contrast is high enough to turn the liquid–liquid interface into a quasisolid–liquid interface. The normalized lifetime of four-phase contact points on the PDMS pseudo-brushes is lower compared to hard silanized surfaces, which means the four-phase contact points are faster on PDMS pseudo-brushes. Since the contact angle and the ratio of surface tension to viscosity are the same for PDMS pseudo-brushes and hard silanized substrates, the difference must be due to the wetting properties of the surfaces. We assume that the low contact angle hysteresis (pinning) of the PDMS pseudo-brushes plays a key role in speeding up the dynamics of the four-phase contact point. The normalized lifetime on PDMS pseudo-brushes is about 35% lower than the normalized life time on silanized surfaces. In the highly viscous first drops, the difference decreases, but the tendency remains the same for all liquid combinations [Fig. 6(b)].

The used PDMS pseudo-brushes differed in thickness (Fig. 3) and viscosity of the used PDMS (Table I). These differences seem to have no influence on the dynamics of the four-phase contact point, as the corresponding data points in Fig. 6 overlap within their uncertainty. We conclude that the dynamics in the pseudo-brush have little influence on the dynamics of the four-phase contact point.

It is beyond the concept of this paper to develop a model to mimic the process entirely. Nevertheless, we will try to qualitatively explain the process. If we follow the same analogy as it presented in the paper,[37] the friction source has two contributors. Force dissipation at liquid–liquid interface as well as liquid–solid interface are these two main sources. The friction at liquid–liquid interface remains constant, but the friction at liquid–solid interface is reduced ten times for PDMS pseudo-brush [Eq. (3)]. This can explain the speeding up of four-phase contact points, but to make a general statement on why the time's exponent is different in this case, further investigations are needed.

VI. CONCLUSION

PDMS pseudo-brushes show specific wetting properties (i.e., low contact angle hysteresis and higher mobility of surface[8,12]). Here, we compare silanized substrates with very similar advancing contact angles that vary in contact angle hysteresis by a factor of 10. This reduction can be explained by the fact that the PDMS pseudo-brushes have lower chemical and topographical roughness (i.e., pinning). We showed this by employing the AFM tapping mode imaging. We measured the thickness of these pseudo-brushes by the x-ray reflectivity (XRR) method. For all measured substrates, the thicknesses of the pseudo-brushes are in the order of a few nanometers. In the last section, we investigated the presence of PDMS pseudo-brush on the dynamics of the four-phase contact point. These pseudo-brushes increase the four-phase contact point speed (compared to the silanized substrate) and change the time dependency of the four-phase contact point. It is shown that the molar mass of used PDMS pseudo-brush (in range of our study) does not have an impact on the wetting properties of pseudo-brushes. The dynamics of the four-phase contact point are controlled, as in a previous study[37] by the ratio of surface tension to the viscosity of the second drop and the first drop.

SUPPLEMENTARY MATERIAL

See the supplementary material for further explanation on the XRR method as well as further experiments on the PDMS pseudo-brushes with the AFM and the XRR methods. A short description of relation of the pseudo-brushes and property of used polymer melt and a comparison between the energy dissipation in these pseudo-brushes and thick PDMS layers are presented.

ACKNOWLEDGMENTS

This study was funded by the Deutsche Forschungsgemeinschaft Project No. 265191195–SFB 1194, "Interaction between Transport and Wetting Processes" and Project Nos. A02, A06, and A09. The authors also wish to thank Stefan Michel for the fruitful discussion.

AUTHOR DECLARATIONS

Conflict of Interest

The authors have no conflicts to disclose.

Author Contributions

Peyman Rostami: Conceptualization (lead); Data curation (lead); Formal analysis (lead); Investigation (lead); Methodology (lead); Software (lead); Validation (lead); Visualization (lead); Writing – original draft (lead); Writing – review & editing (lead). **Mohammad Ali Hormozi**: Conceptualization (lead); Data curation (lead); Formal analysis (lead); Investigation (lead); Methodology (lead); Visualization (lead); Writing – original draft (lead). **Olaf Soltwedel**: Data curation (equal); Formal analysis (equal); Investigation (equal); Methodology (equal); Validation (equal); Visualization (equal); Writing – original draft (equal). **Reza Azizmalayeri**: Methodology (equal); Writing – review & editing (equal). **Regine von Klitzing**: Funding acquisition (equal); Resources (equal); Supervision (equal); Writing – review & editing (equal). **Günter K. Auernhammer**: Conceptualization (equal); Funding acquisition (equal); Methodology (equal); Project administration (equal); Resources (equal); Supervision (equal); Writing – review & editing (equal).

DATA AVAILABILITY

The data that support the findings of this study are available from the corresponding author upon reasonable request.

REFERENCES

[1]B. Zhao and W. J. Brittain, "Polymer brushes: Surface-immobilized macromolecules," Prog. Polym. Sci. **25**, 677–710 (2000).
[2]O. Guiselin, "Irreversible adsorption of a concentrated polymer-solution," Europhys. Lett. **17**, 225–230 (1992).
[3]M. Aubouy, O. Guiselin, and E. Raphaël, "Scaling description of polymer interfaces: Flat layers," Macromolecules **29**, 7261–7268 (1996).
[4]J. W. Krumpfer and T. J. McCarthy, "Rediscovering silicones: 'Unreactive' silicones react with inorganic surfaces," Langmuir **27**, 11514–11519 (2011).
[5]S. T. Milner, "Polymer brushes," Science **251**, 905–914 (1991).
[6]P. G. de Gennes, "Conformations of polymers attached to an interface," Macromolecules **13**, 1069–1075 (1980).
[7]H. Yong, E. Bittrich, P. Uhlmann, A. Fery, and J.-U. Sommer, "Co-nonsolvency transition of poly(*N*-isopropylacrylamide) brushes in a series of binary mixtures," Macromolecules **52**, 6285–6293 (2019).
[8]R. Lhermerout, H. Perrin, E. Rolley, B. Andreotti, and K. Davitt, "A moving contact line as a rheometer for nanometric interfacial layers," Nat. Commun. **7**, 12545 (2016).
[9]H. Zeng, J. Huang, Y. Tian, L. Li, M. V. Tirrell, and J. N. Israelachvili, "Adhesion and detachment mechanisms between polymer and solid substrate surfaces: Using polystyrene–mica as a model system," Macromolecules **49**, 5223–5231 (2016).
[10]J. Klein, E. Kumacheva, D. Mahalu, D. Perahia, and L. J. Fetters, "Reduction of frictional forces between solid surfaces bearing polymer brushes," Nature **370**, 634–636 (1994).
[11]M. Kim, S. Schmitt, J. Choi, J. Krutty, and P. Gopalan, "From self-assembled monolayers to coatings: Advances in the synthesis and nanobio applications of polymer brushes," Polymers **7**, 1346–1378 (2015).
[12]A. Eifert, D. Paulssen, S. N. Varanakkottu, T. Baier, and S. Hardt, "Simple fabrication of robust water-repellent surfaces with low contact-angle hysteresis based on impregnation," Adv. Mater. Interfaces **1**, 1300138 (2014).
[13]J. W. Krumpfer and T. J. McCarthy, "Contact angle hysteresis: A different view and a trivial recipe for low hysteresis hydrophobic surfaces," Faraday Discuss. **146**, 103–111 (2010).
[14]R. Lhermerout and K. Davitt, "Contact angle dynamics on pseudo-brushes: Effects of polymer chain length and wetting liquid," Colloids Surf., A **566**, 148–155 (2019).
[15]D. F. Cheng, C. Urata, M. Yagihashi, and A. Hozumi, "A statically oleophilic but dynamically oleophobic smooth nonperfluorinated surface," Angew. Chem. **124**, 3010–3013 (2012).
[16]D. F. Cheng, C. Urata, B. Masheder, and A. Hozumi, "A physical approach to specifically improve the mobility of alkane liquid drops," J. Am. Chem. Soc. **134**, 10191–10199 (2012).
[17]J. F. Joanny and P. G. de Gennes, "A model for contact angle hysteresis," J. Chem. Phys. **81**, 552–562 (1984).
[18]J. D. Miller, S. Veeramasuneni, J. Drelich, M. R. Yalamanchili, and G. Yamauchi, "Effect of roughness as determined by atomic force microscopy on the wetting properties of PTFE thin films," Polym. Eng. Sci. **36**, 1849–1855 (1996).
[19]N. Rangelova, V. Izmailova, D. Platikanov, G. Yampol'skaya, and Z. Tulovskaya, "Free black films of proteins: Dynamic hysteresis of the contact angle (film-bulk liquid) and the rheological properties of adsorption layers," Colloid J. USSR **52**, 442–447 (1990).
[20]N. V. Churaev, B. V. Derjaguin, and V. M. Muller, *Surface Forces* (Springer Science & Business Media, 2013).
[21]H. Hu and Y. Sun, "Molecular dynamics simulations of disjoining pressure effect in ultra-thin water film on a metal surface," Appl. Phys. Lett. **103**, 263110 (2013).
[22]M. Delmas, M. Monthioux, and T. Ondarçuhu, "Contact angle hysteresis at the nanometer scale," Phys. Rev. Lett. **106**, 136102 (2011).
[23]C. W. Extrand, "Contact angles and hysteresis on surfaces with chemically heterogeneous islands," Langmuir **19**, 3793–3796 (2003).
[24]B. Andreotti and J. H. Snoeijer, "Statics and dynamics of soft wetting," Annu. Rev. Fluid. Mech. **52**, 285–308 (2020).
[25]L. Chen, G. K. Auernhammer, and E. Bonaccurso, "Short time wetting dynamics on soft surfaces," Soft Matter **7**, 9084–9089 (2011).
[26]S. Karpitschka, S. Das, M. van Gorcum, H. Perrin, B. Andreotti, and J. H. Snoeijer, "Droplets move over viscoelastic substrates by surfing a ridge," Nat. Commun. **6**, 7891 (2015).
[27]X. Sui, S. Zapotoczny, E. M. Benetti, P. Schön, and G. J. Vancso, "Characterization and molecular engineering of surface-grafted polymer brushes across the length scales by atomic force microscopy," J. Mater. Chem. **20**, 4981–4993 (2010).
[28]S. Sakurai, H. Watanabe, and A. Takahara, "Preparation and characterization of looped polydimethylsiloxane brushes," Polym. J. **46**, 117–122 (2014).
[29]S. Vlassov, S. Oras, M. Antsov, I. Sosnin, B. Polyakov, A. Shutka, M. Y. Krauchanka, and L. M. Dorogin, "Adhesion and mechanical properties of PDMS-based materials probed with AFM: A review," Rev. Adv. Mater. Sci. **56**, 62–78 (2018).
[30]R. Barbey, L. Lavanant, D. Paripovic, N. Schüwer, C. Sugnaux, S. Tugulu, and H.-A. Klok, "Polymer brushes via surface-initiated controlled radical polymerization: Synthesis, characterization, properties, and applications," Chem. Rev. **109**, 5437–5527 (2009).
[31]G. Sudre, E. Siband, B. Gallas, F. Cousin, D. Hourdet, and Y. Tran, "Responsive adsorption of *N*-isopropylacrylamide based copolymers on polymer brushes," Polymers **12**, 153 (2020).
[32]B. Voigtländer, *Atomic Force Microscopy* (Springer, 2019).
[33]M. Motornov, R. Sheparovych, I. Tokarev, Y. Roiter, and S. Minko, "Nonwettable thin films from hybrid polymer brushes can be hydrophilic," Langmuir **23**, 13–19 (2007).
[34]M. Brik, S. Harmand, I. Zaaroura, and A. Saboni, "Experimental and numerical study for the coalescence dynamics of vertically aligned water drops in oil," Langmuir **37**, 3139–3147 (2021).
[35]J. Jin, C. Ooi, D. Dao, and N.-T. Nguyen, "Coalescence processes of droplets and liquid marbles," Micromachines **8**, 336 (2017).
[36]T. M. Dreher, J. Glass, A. J. O'Connor, and G. W. Stevens, "Effect of rheology on coalescence rates and emulsion stability," AIChE J. **45**, 1182–1190 (1999).
[37]P. Rostami and G. K. Auernhammer, "Capillary filling in drop merging: Dynamics of the four-phase contact point," Phys. Fluids **34**, 012107 (2022).
[38]L. Mahadevan, M. Adda-Bedia, and Y. Pomeau, "Four-phase merging in sessile compound drops," J. Fluid Mech. **451**, 411–420 (2002).
[39]R. Lucas, "Ueber das zeitgesetz des kapillaren aufstiegs von flüssigkeiten," Kolloid-Z. **23**, 15–22 (1918).
[40]E. W. Washburn, "The dynamics of capillary flow," Phys. Rev. **17**, 273 (1921).
[41]R. R. Rye, J. A. Mann, and F. G. Yost, "The flow of liquids in surface grooves," Langmuir **12**, 555–565 (1996).
[42]See https://www.gelest.com/product for Gelest product properties.
[43]H. Teisala, P. Baumli, S. A. L. Weber, D. Vollmer, and H.-J. Butt, "Grafting silicone at room temperature—A transparent, scratch-resistant nonstick molecular coating," Langmuir **36**, 4416–4431 (2020).
[44]R. A. Brown, F. M. Orr, Jr., and L. E. Scriven, "Static drop on an inclined plate: Analysis by the finite element method," J. Colloid Interface Sci. **73**, 76–87 (1980).
[45]C. W. Extrand and A. N. Gent, "Retention of liquid drops by solid surfaces," J. Colloid Interface Sci. **138**, 431–442 (1990).
[46]C. W. Extrand and Y. Kumagai, "Liquid drops on an inclined plane: The relation between contact angles, drop shape, and retentive force," J. Colloid Interface Sci. **170**, 515–521 (1995).
[47]E. Wolfram and R. Faust, "Liquid drops on a tilted plate: Contact angle hysteresis and the Young contact angle," in *Wetting, Spreading and Adhesion*, edited by J. F. Padday (Academic Press, London, 1978), pp. 213–222.
[48]E. B. Dussan V., "On the ability of drops to stick to surfaces of solids. Part 3. The influences of the motion of the surrounding fluid on dislodging drops," J. Fluid Mech. **174**, 381–397 (1987).
[49]A. I. ElSherbini and A. M. Jacobi, "Retention forces and contact angles for critical liquid drops on non-horizontal surfaces," J. Colloid Interface Sci. **299**, 841–849 (2006).
[50]F. Henrich, D. Fell, D. Truszkowska, M. Weirich, M. Anyfantakis, T.-H. Nguyen, M. Wagner, G. K. Auernhammer, and H.-J. Butt, "Influence of surfactants in forced dynamic dewetting," Soft Matter **12**, 7782–7791 (2016).